ISSN 0015-4628, Fluid Dynamics, 2019, Vol. 54, No. 1, pp. 42–55. © Pleiades Publishing, Ltd., 2019.
Russian Text © The Author(s), 2019, published in Izvestiya Rossiiskoi Akademii Nauk, Mekhanika Zhidkosti i Gaza, 2019, No. 1, pp. 44–57.

Analysis of the Shape Hysteresis of a Soap Film Supported by Two Circular Rings

M. M. Alimov[1]* and K. G. Kornev[2]

[1]*Kazan (Privolzhskii) Federal University, Kazan, Russia*

[2]*Clemson University, Clemson, SC, USA*

Received March 12, 2018; in final form, June 14, 2018; accepted June 20, 2018

Abstract—The behavior of a minimal surface supported by two circular coaxial rings is analyzed by increasing (decreasing) distance between rings. The assumption on metastability of certain configurations of the minimal surface is confirmed. This makes it possible to explain hysteresis of a soap film taking on different configurations observed experimentally. The effectiveness of applying analytical methods of the theory of flows of Non-Newtonian fluids through porous media to the problem of describing minimal surfaces on rings is demonstrated.

Key words: minimal surfaces, catenoid, stability, complex variables.

DOI: 10.1134/S0015462819010026

The films on various frames pulled out of a soap solution represent the minimal surfaces whose shape is determined by the condition of the surface energy minimum or, in fact, the condition of the surface area minimum [1]. Despite the dear physical mechanism, the rich history of the problem dating back to the reference [2], and the great number of mathematical investigations devoted to this problem (see [3–5] and the references there in), the behavior of films on frames can be predicted only in the very simple cases. In particular, this is the case of the circular, identical, and coaxial rings for which the minimal surface represents the surface of revolution whose profile is a catenary curve. Such a minimal surface is called catenoid [4] and its complete analysis can be found, for example, in [6].

It should be noted that even in this simplest case the behavior of the minimal surface is not trivial. Instead of the regular catenoid, i.e., an everywhere smooth surface with a narrow neck in its middle part, the catenoids with a planar film in the neck can be observed sometimes. Such a catenoid will be already singular, since it represents the set of three smooth segments which meet along a certain line, namely, a singular rib of the minimal surface [4].

If we take two circular rings of different radii, then the film forms an asymmetric catenoid, namely, its neck will be located not in the middle part. The experiments demonstrated that this asymmetry can lead to unexpected results in the behavior of the film: as the distance between the rings increases (decreases), the regular asymmetric catenoid changes its shape and becomes singular and back and, moreover, the direct and reverse shape reconstructions occur at different distances, i.e., there is hysteresis in reconstruction of the film shape [7].

Drawing an analogy with the reconstruction of minimal surfaces and the phase transitions, the authors of [7] suggested that one of the possible film configurations on such a system of rings is metastable. This made it possible to explain the hysteresis itself. However, in [7] no estimations of the surface energy corresponding to various configurations of the catenoid have been provided. Hence, this hypothesis was not proved.

The present study has the double aim. First, it aims to explain the experimental results obtained in [7] by carrying out the complete analysis of the behavior of minimal surfaces on the system of two circular coaxial rings of different diameters. Second, it aims to propose a new method for analysis of configurations of minimal surfaces on frames using an analogy with the theory of flows of Non-Newtonian fluids through porous media [9] revealed in [8]. While the theory applied directly to a catenoid

*E-mail: Mars.Alimov@kpfu.ru.

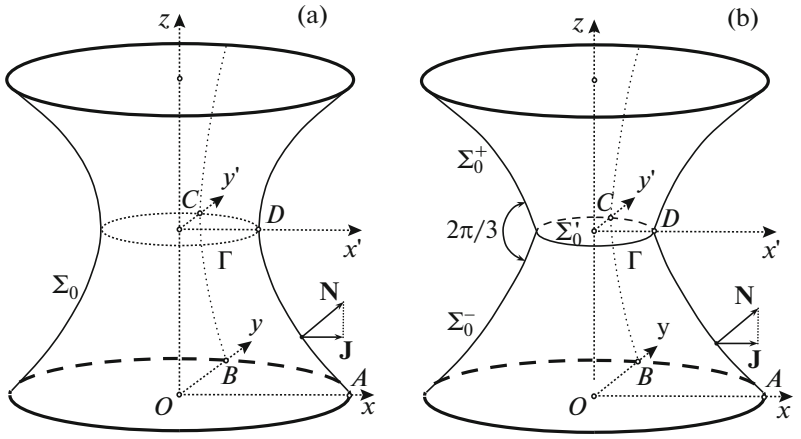

Fig. 1. Symmetric regular catenoid Σ_0 (a) and symmetric singular catenoid $\Sigma_0^+ \bigcup \Sigma_0^- \bigcup \Sigma_0'$, i.e., the catenoid with the planar film Σ_0' in the neck (b).

is somewhat more complex as compared to the classical method [6] it is advantageous as it can be extended to non-circular and non-smooth frames.

First, we will consider the case of identical circular rings and, respectively, symmetric regular and singular catenoids.

1. FORMULATION OF THE PROBLEM OF SYMMETRIC CATENOID

We will take the ring radius as the characteristic length. Adopting the notation R_{up} and R_{dn} for the upper and lower ring radii, respectively, we can set

$$R_{dn} = R_{up} = 1.$$

We will assume that the ring planes are horizontal and the plane of the lower ring is the x, y plane. The z axis directed vertically upward will be the axis of symmetry of the rings. In Figs. 1a and 1b we have schematically reproduced, respectively, a regular catenoid, which represents smooth surface Σ_0, and, respectively, a singular catenoid as the set of smooth segments $\Sigma_0^+ \bigcup \Sigma_0^- \bigcup \Sigma_0'$, where Σ_0' is the circular plane film in the catenoid neck.

Being the surface of revolution, the symmetric catenoid possesses also symmetry about the horizontal plane $x'y'$ which passes through the geometric center of catenoid. Therefore, for both regular and singular catenoids it is sufficient to restore the configuration of an element of symmetry of the minimal surface, for example, of its segment $ABCDA$, see Figs. 1a and 1b.

The configuration of segment $ABCDA$ of the minimal surface can be specified as a function of the height of a point (x, y, z) of the minimal surface above the xy plane

$$z = h(x, y).$$

This function is defined in the domain Ω which is the projection of the element of symmetry $ABCDA$ of the minimal surface on the xy plane, see Fig. 2a.

For finding the function $h(x, y)$ it is necessary to solve the boundary-value problem

$$\Omega: \quad \nabla\left[\left(1 + |\nabla h|^2\right)^{-1/2} \nabla h\right] = 0, \tag{1.1}$$

$$AD: \quad \frac{\partial h}{\partial y} = 0, \tag{1.2}$$

$$BC: \quad \frac{\partial h}{\partial x} = 0, \tag{1.3}$$

$$AB: \quad h = 0, \tag{1.4}$$

$$\Gamma: \quad h = \frac{l_0}{2}, \quad |\nabla h| \to \infty, \tag{1.5}$$

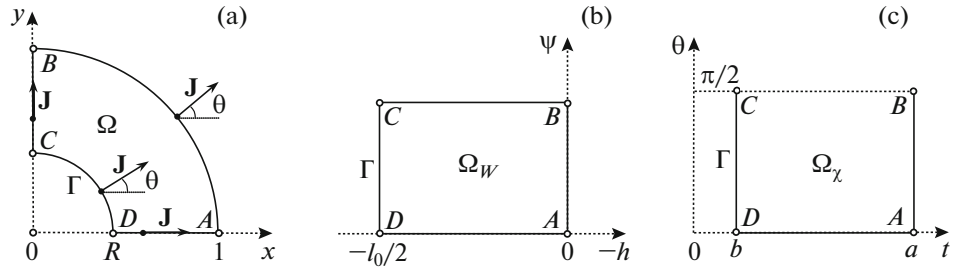

Fig. 2. Views of the flow region in the x, z plane (a), in the plane of the complex potential W (b), and in the plane of the velocity hodograph χ (c) for the symmetric catenoid.

or

$$\Gamma: \quad h = \frac{l_0}{2}, \quad \left(1 + |\nabla h|^2\right)^{-1/2} |\nabla h| = \cos\left(\frac{\pi}{6}\right). \tag{1.6}$$

Here, equation (1.1) is the differential equation of the minimal surface [3], (1.2) and (1.3) are the conditions of smooth symmetric continuation of the function $h(x, y)$ and, consequently, also of the minimal surface Σ_0 across the boundaries AD and BC, respectively; and (1.4) is the boundary condition of the lower ring.

In both cases, the boundary $\Gamma = CD$ is the cross-section of the neck of the minimal surface Σ_0 by the horizontal middle plane $x'y'$ (see Fig. 1a). In the singular case, in addition, this is the singular rib of the surface $\Sigma_0^+ \bigcup \Sigma_0^- \bigcup \Sigma_0'$ (see Fig. 1b). In both cases, the boundary Γ is a circle, its radius R is unknown and formally it is the free boundary. Therefore, two conditions (1.5) must be specified on it in the regular case and, respectively, two conditions (1.6) must be specified in the singular case. In (1.5) and (1.6) the first of the conditions represent the conditions of constant height $h(x, y)$. For the regular catenoid the second of the conditions in (1.5) reflects the fact of orthogonality of the plane $x'y'$ and the minimal surface Σ_0.

For the singular catenoid the angle between each of the pairs of the segments Σ_0^+, Σ_0^-, and Σ_0' on their joining line Γ must be equal to $2\pi/3$ [4] and, consequently, the normal $\mathbf{N}$ to the minimal surface will form the angle of $\pi/6$ with the horizontal plane $x'y'$. Just this fact reflects the second of the conditions in (1.6) for the singular catenoid, since the quantity $\left(1 + |\nabla h|^2\right)^{-1/2} |\nabla h|$ represents the projection of $\mathbf{N}$ on the $x'y'$ plane [10].

Thus, for determining the configuration of symmetric regular catenoid it is necessary to solve the boundary-value problem (1.1)–(1.5) and for determining the configuration of symmetric singular catenoid it is necessary to solve the boundary-value problem (1.1)–(1.4), (1.6). The distance between the loop planes l_0 represents the single governing parameter of the problem on which the configuration of the minimal surface depends.

2. ANALOGY WITH THE THEORY OF FLOWS OF NON-NEWTONIAN FLUIDS THROUGH POROUS MEDIA

In [8] it was established that an analogy with the problems of anomalous viscous fluid flow through porous media [9] can be effectively used to analyze the problems of the minimal surface. We define the fictitious hydrodynamic fluid flux $\mathbf{J}$ as follows:

$$\mathbf{J} = -\frac{\nabla h}{|\nabla h|} J, \quad J = \frac{|\nabla h|}{\sqrt{1 + |\nabla h|^2}}. \tag{2.1}$$

The flux vector $\mathbf{J}$ can be characterized by its absolute value $J = |\mathbf{J}|$ and the angle θ of inclination to the x axis. Relation (2.1) between the quantities J and $|\nabla h|$ can be written in the other form:

$$|\nabla h| = \Phi(J), \quad \Phi(J) = J(1 - J^2)^{-1/2}, \tag{2.2}$$

where $\Phi(J) \geq 0$ and $\Phi'(J) \geq 0$. Accordingly, the differential equation (1.1) makes it possible to introduce fictitious anomalous fluid flow through the porous media [9]

$$\Omega: \quad \nabla h = -\frac{\mathbf{J}}{J}\Phi(J), \quad \nabla \mathbf{J} = 0. \tag{2.3}$$

In this case $h(x, y)$ is an analog of the head and $\mathbf{J}(x, y)$ is an analog of the seepage velocity. In Fig. 2a we have reproduced the view of flow. The seepage flow law (2.2) was first considered by Sokolovskii [11].

The second of the differential equations (2.3) means that fluid is incompressible and, consequently, we can introduce the streamline function $\psi(x, y)$ [12]. Then

$$J_x = J\cos\theta = \frac{\partial \psi}{\partial y}, \quad J_y = J\sin\theta = -\frac{\partial \psi}{\partial x}.$$

As shown by Khristianovich [13], for flows through porous media which must satisfy the law (2.3), it is reasonably to use the Chaplygin transformation [14] in respect to variables of the velocity hodograph t, θ. For the Sokolovskii law (2.2) the variable t will relate to J by the expression [11]

$$J = \cosh^{-1} t, \quad t = \operatorname{arccosh} J^{-1}, \quad \Phi(J) = \sinh^{-1} t. \tag{2.4}$$

As a result of such a transformation, we arrive at the Cauchy–Riemann relation (details see in [11, 15]):

$$\frac{\partial \psi}{\partial t} = \frac{\partial h}{\partial \theta}, \quad \frac{\partial \psi}{\partial \theta} = -\frac{\partial h}{\partial t}.$$

Consequently, we can introduce the complex variables W and χ

$$W = -h + i\psi, \quad \chi = t + i\theta$$

and use the functions of complex variable $\chi(W)$ or $W(\chi)$ [16]. Conventionally, W is called the complex flow potential and χ is called the velocity hodograph [9].

When the function $\chi(W)$ will be found, we can return to the physical plane x, y by writing the Khristianovich formulas of the total differentials for the functions $x(h, \psi)$ and $y(h, \psi)$ [9, 13]

$$dx = -\cos\theta \sinh t dh - \sin\theta \cosh t d\psi, \quad dy = -\sin\theta \sinh t dh + \cos\theta \cosh t d\psi. \tag{2.5}$$

As shown in [9], the problem of determination of the function $\chi(W)$ can be effectively solved using the velocity hodograph method [17] under the condition that the planes χ and W have the canonical form.

3. ANALYSIS OF THE FORM OF COMPLEX POTENTIAL AND VELOCITY HODOGRAPH PLANES

Initially, we will analyze the form of the plane of the complex potential $W = -h + i\psi$. The boundaries AD and BC of the domain Ω are the streamlines (see Fig. 2a) and the boundaries AB and CD are the lines of constant h (see formulas (1.4)–(1.6)). Therefore, in the plane of the potential $W = -h + i\psi$ the flow domain Ω corresponds to the rectangular Ω_W represented in Fig. 2b.

In order to analyze the form of the plane of the velocity hodograph $\chi = t + i\theta$, in addition to the representation of $\mathbf{J}$ as the vector of incompressible fluid flux, it is convenient also to use its geometric interpretation: in accordance with [10], the flux vector $\mathbf{J}(x, y)$ of form (2.1) will be the projection of the normal vector $\mathbf{N}(x, y)$ on the plane x, y (see Fig. 1).

With regard to the flow pattern (see Fig. 2a), we have on the streamlines AD and BC:

$$AD: \quad \theta = 0; \quad BC: \quad \theta = \frac{\pi}{2}. \tag{3.1}$$

On the boundaries AB and CD we will use the fact that the normal vector $\mathbf{N}(x, y)$ is orthogonal to the boundaries themselves. Then the flux vector $\mathbf{J}$ will be orthogonal to them (see Fig. 2a). Then, from considerations of axial symmetry of flow it follows that the absolute value of the flux J will be constant on each of the boundaries AB and CD.

On the boundary $\Gamma = CD$ in the regular case the absolute value of the flux J can be found from the second of the boundary conditions in (1.5), namely, $J = 1$ and, respectively, in the singular case from

the boundary condition (1.6): $J = \cos(\pi/6)$. In the regular and singular cases, for the parameter b we introduce the notation b_r, b_s, respectively:

$$b = \begin{cases} b_r = 0, \\ b_s = \operatorname{arccosh}\left[\cos^{-1}\left(\dfrac{\pi}{6}\right)\right]. \end{cases} \tag{3.2}$$

Then with regard to the relation (2.4) between J and t, in both cases the condition on Γ can be written in the general form:

$$\Gamma: \quad t = b \quad \Leftrightarrow \quad J = \cosh^{-1} b. \tag{3.3}$$

On the boundary AB the flux J is constant but its value is unknown. As a result of the same formula (2.4), on the boundary AB the value of t will be also constant but indefinite. We will denote it by a

$$AB: \quad t = a \quad \Leftrightarrow \quad J = \cosh^{-1} a. \tag{3.4}$$

Taking formulas (3.1)–(3.4) into account, we can conclude that the rectangular Ω_χ given in Fig. 2c corresponds to the flow domain Ω in the velocity hodograph plane χ. The parameter a determining the rectangular side ratio will be the main auxiliary parameter of the problem. Obviously that $a > b$.

Taking into account the form of the complex planes $W = -h + i\psi$ and $\chi = t + i\theta$, we can readily find the conformal mapping $W(\chi)$

$$W(\chi) = \frac{l_0}{2(a-b)}(\chi - a),$$

which directly determines the functions $h(t,\theta)$ and $\psi(t,\theta)$:

$$h(t,\theta) = -\frac{l_0}{2(a-b)}t + \frac{al_0}{2(a-b)}, \quad \psi(t,\theta) = \frac{l_0}{2(a-b)}\theta. \tag{3.5}$$

4. RECONSTRUCTION OF THE CONFIGURATION OF THE MINIMAL SURFACE

The radius R of the circle Γ can be determined from considerations of the material balance. In fact, by virtue of incompressibility of fluid its total fluxes across the boundaries AB and CD must coincide. The vector $\mathbf{J}$ is orthogonal to the boundaries and its absolute value j is constant on each of the boundaries. Taking this fact into account, we have

$$2\pi R J|_\Gamma = 2\pi J|_{AB}.$$

As a result, using conditions (3.3) and (3.4), we obtain

$$R = \frac{\cosh b}{\cosh a}. \tag{4.1}$$

The configuration of the entire minimal surface can be found by determining the function $h(x,y)$. Since the problem was parameterized by introducing the auxiliary plane $\chi = t + i\theta$, the function $h(x,y)$ is indirectly determined by the functions $h(t,\theta)$, $x(t,\theta)$, and $y(t,\theta)$. The function $h(t,\theta)$ is already known (see formula (3.5)). In order to find the functions $x(t,\theta)$ and $y(t,\theta)$, we will use the Khristianovich differential formulas of the general form (2.5). Substituting the expressions for the partial derivatives of the functions $h(t,\theta)$ and $\psi(t,\theta)$ following from (3.5)

$$\frac{\partial h}{\partial t} = -\frac{l_0}{2(a-b)}, \quad \frac{\partial h}{\partial \theta} = 0; \quad \frac{\partial \psi}{\partial t} = 0, \quad \frac{\partial \psi}{\partial \theta} = \frac{l_0}{2(a-b)},$$

we obtain the formulas

$$dx = \frac{l_0}{2(a-b)}\left[\cos\theta \sinh t dt - \sin\theta \cosh t d\theta\right], \quad dy = \frac{l_0}{2(a-b)}\left[\sin\theta \sinh t dt + \cos\theta \cosh t d\theta\right]. \tag{4.2}$$

In particular, for the boundary Γ from formulas (4.2) with regard to condition (3.3) there follows

$$\Gamma: \quad dx = -\frac{l_0 \cosh b}{2(a-b)} \sin\theta d\theta, \quad dy = \frac{l_0 \cosh b}{2(a-b)} \cos\theta d\theta.$$

Correspondingly, we can relate the increments of the arc abscissa s_Γ of the boundary Γ and the angle θ of inclination of the normal to this boundary to the x axis

$$\Gamma: \quad ds_\Gamma = \sqrt{(dx)^2 + (dy)^2} = \frac{l_0 \cosh b}{2(a-b)} d\theta.$$

Since Γ is the circle, from the last expression there follows another formula for the radius R of the circle Γ

$$R = \frac{l_0 \cosh b}{2(a-b)}.$$

Comparing this formula with formula (4.1), we obtain the relation of the single governing parameter of the problem l_0 with the main auxiliary parameter of the problem a

$$l_0(a) = 2\left(\frac{a-b}{\cosh a}\right). \tag{4.3}$$

Then, using formulas (4.2) of the differentials of the functions $x(t,\theta)$ and $y(t,\theta)$, we can reconstruct also the functions themselves; however, since both regular and singular catenoids are the surfaces of revolution, it is sufficient to establish their profile in the xz plane as a function $x = x(z)$. For the boundary AD from formulas (4.2) with regard to the first of the conditions (3.1) and formula (4.3) we can obtain the relation connecting the differentials of t and x

$$AD: \quad dx = \frac{l_0 \sinh t}{2(a-b)} dt = \frac{\sinh t}{\cosh a} dt.$$

We will integrate this equation from point D at which $t = b$ and $x = R$. Taking expression (4.1) into account, we can find the function $x(t)$ on the boundary AD

$$AD: \quad x(t) = \frac{\cosh t}{\cosh a}. \tag{4.4}$$

In reality, the function $z(t)$ on the boundary AD is given by the first of the expressions in formula (3.5). Taking expression (4.3) into account, we can write it as follows:

$$AD: \quad z = \frac{a-t}{\cosh a}.$$

Inverting the function $z(t)$, we can find the function $t(z)$ on the boundary AD

$$AD: \quad t(z) = a - z\cosh a. \tag{4.5}$$

Substituting formula (4.5) in formula (4.4), we obtain the unknown profile $x(z)$ of the boundary AD

$$AD: \quad x(z) = \frac{\cosh(a - z\cosh a)}{\cosh a}. \tag{4.6}$$

This profile is the catenary curve and differs from the well-known formulas [6] by only the choice of the origin and the scale.

5. DETERMINATION OF THE MINIMAL SURFACE AREA

The part of catenoid between the planes $z = 0$ and $z = z'$ represents the surface of revolution with the given profile $x(z)$ and the axis of rotation z. Therefore, for calculating its area $S(z')$ we can use the following formula [18]

$$S(z') = 2\pi \int_0^{z'} x(z)\sqrt{1 + \left(\frac{dx}{dz}\right)^2}\, dz. \tag{5.1}$$

The profile $x(z)$ is given by expression (4.6). Its direct differentiation yields the expression for dx/dz

$$AD: \quad \frac{dx}{dz} = -\sinh(a - z\cosh a).$$

Substituting it in formula (5.1) and carrying out integration, we obtain

$$S(z') = \pi \frac{2z'\cosh a - \sinh(2a - 2z'\cosh a) + \sinh(2a)}{2\cosh^2 a}. \tag{5.2}$$

Then, in both regular and singular cases, the area of the entire catenoid can be expressed by the single formula

$$S_0 = 2S(z')|_{z'=l_0/2} + \left(bb_s^{-1}\right)\pi R^2. \tag{5.3}$$

Here, the second term underlines that the area of the singular catenoid differs from the area of the regular catenoid by not only another value of b in formula (4.3) for l_0, but also addition of the film area Σ_0' in the catenoid neck. Calculating by means of formula (5.3) with regard to the expressions (4.3) and (5.2), we find the area of symmetric catenoid S_0 as a function of the parameter a

$$S_0(a) = \pi \frac{2(a - b) + \sinh(2a) - \sinh(2b) + \left(bb_s^{-1}\right)\cosh^2 b}{\cosh^2 a}. \tag{5.4}$$

Here, in the regular and singular cases it is necessary to take its own value of b in accordance with formula (3.2).

6. ANALYSIS OF THE RESULTS FOR SYMMETRIC CATENOID

In Fig. 3a we have reproduced the dependence $l_0(a)$ calculated from formula (4.3): curves *1* and *2* correspond to the regular and singular catenoids, respectively. Both curves are nonmonotonic and have maxima marked by asterisks: for curve *1* this is the critical value $l_{0,r}^* = 1.3255$ reached at a equal to $a_r^* = 1.1997$, for curve *2* this is the critical value $l_{0,s}^* = 0.8156$ reached at a equal to $a_s^* = 1.6293$. Consequently, in both regular and singular cases no connected configuration of the minimal surface exists for l_0 larger then the critical value and two configurations of catenoid are possible for l_0 smaller then the critical value.

In Fig. 3b we have reproduced the dependence $R(a)$ calculated from formula (4.1): curves *1* and *2* correspond to the regular and singular catenoids, respectively. The asterisks mark the critical values of R: for curve *1* this is the value equal to $R_r^* = 0.5524$ at $a = a_r^*$ and for curve *2* this is the value equal to $R_s^* = 0.4360$ at $a = a_s^*$. We can see that in both cases the dependence $R(a)$ decreases monotonically and, respectively, two configurations of catenoid mentioned above can be distinguished on the basis of the value of R of the circle Γ, namely, when the parameter a is smaller than the critical value, this is the external catenoid with R greater than the critical value; when the parameter a is greater than the critical value, this is the internal catenoid with R smaller than the critical value.

It is well known that in both regular and singular cases only the external catenoid is stable, since it corresponds to the free energy minimum [6]. In order to make sure of this fact, we reproduce the catenoid surface area S_0 as a function of the distance between the rings l_0 calculated from formula (5.4) (see Fig. 3c). Continuous curves *1* and *2* correspond to the stable branches and curves *1′* and *2′* to the unstable branches of the regular and singular catenoids, respectively. The asterisks mark the critical values at which the dependences $S_0(l_0)$ have cuspidal points. They correspond to $l_0 = l_{0,r}^*$ and

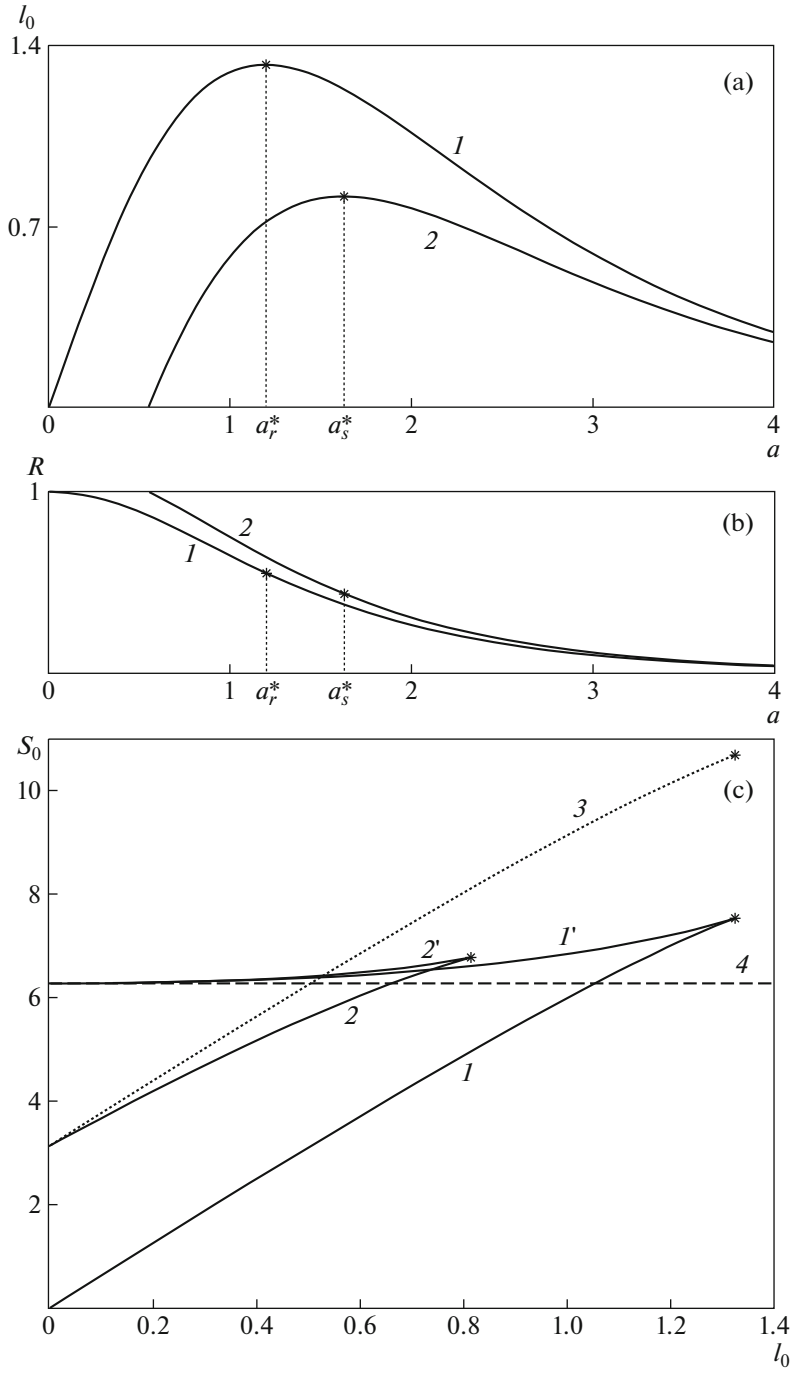

Fig. 3. Quantities l_0 (a) and R (b) as functions of the parameter a for the symmetric catenoid in the regular and singular cases (curves *1* and *2*, respectively). The symmetric catenoid area S_0 as a function of l_0 (c): curves *1* and *2* correspond to the external (stable) configuration of catenoid and curves *1′* and *2′* to the internal (unstable) configuration of catenoid in the regular and singular cases, respectively; curve *3* corresponds to the stable state of the "regular catenoid with film on one of the rings" system, and curve *4* corresponds to two individual films on the rings.

$S_0 = S_{0,r}^* = 7.5378$ in the regular case and $l_0 = l_{0,s}^*$ and $S_0 = S_{0,s}^* = 6.7856$ in the singular case. Broken curve *4* denotes the solution $S_0 = 2\pi$ which corresponds to the case of discontinuous solution of the problem, namely, two individual films on the rings.

In this connection, the question of the possibility of reconstructing of a regular catenoid in a singular one and vice versa arises. Restricting our attention to consideration of only the stable configurations

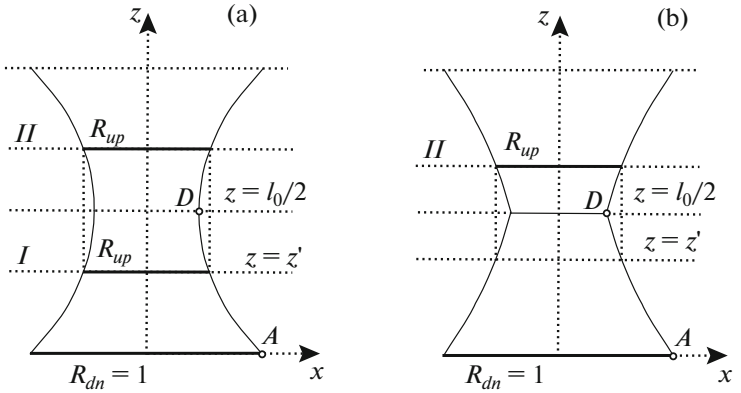

Fig. 4. Diagram of determination of the asymmetric catenoid on the basis of a given value of $R_{up} < 1$ by means of the cross-section of the symmetric catenoid Σ_0 in the regular case (a) and $\Sigma_0^+ \bigcup \Sigma_0^- \bigcup \Sigma_0'$ in the singular case (b): solutions *I* and *II* correspond to the catenoids without and with the neck, respectively.

of the external catenoid (see curves *1* and *2* in Fig. 3c), we can conclude that the area of the singular catenoid is always greater than the area of the regular catenoid at a fixed l_0. Therefore, the regular catenoid cannot be spontaneously reconstructed in the singular one. The question remains: does the reconstruction be possible?

If the distance between the rings l_0 is greater than $l_{0,s}^*$, then, obviously, the catenoid cannot remain singular and, in particular, can become regular if the middle film Σ_0' collapses. However, this is only a single of the probable outcomes and other outcomes are possible: for example, transition of the system to discontinuous solution, namely, two individual films on each ring, or to collapse of all the films.

At the same time, if the distance between the rings l_0 is smaller than $l_{0,s}^*$, then, at the first glance, it seems that for the system it is more energetically profitable to go over from the singular catenoid to the regular one. However, this is not true since there is a middle film Σ_0' on the catenoid. If we reject the possibility of its removal by means of external interference, then for such a transition it is necessary that film Σ_0' goes over on one of the rings. Obviously, the free energy of such a system, namely, "regular catenoid plus a film on the ring," will be already characterized not simply by the area $S_{0,r}$ of the regular catenoid in the stable external configuration (curve *1*) but by the sum $(S_{0,r} + \pi)$ (see curve *3* in Fig. 3c). This curve passes already above the singular catenoid in the stable external configuration (curve *2*) and transition from the singular catenoid to the "regular catenoid plus a film on the ring" system is not possible.

We will also consider the inverse situation when the film is additionally "planted" on one of the rings to the regular catenoid. If the distance between the rings l_0 is greater than $l_{0,s}^*$, then the system will remain in the same state, since for such l_0 there is no alternative (singular catenoid). However, if at the instant of planting the distance between the rings l_0 is smaller than $l_{0,s}^*$, the added film will slide down to the neck of the regular catenoid and the system will go over from the "regular catenoid with a film on one of the rings" state to the singular catenoid.

As noted in [7], such a reconstruction of catenoid occurs at two stages, namely, initially the film slides down from the ring to the catenoid neck and then the catenoid, which has already become singular, arrives at the equilibrium state. Correspondingly, the necessary condition of this reconstruction is not only more profitable final state (with the lower free energy), but also the more profitable intermediate state after sliding down the film in the catenoid neck. Here, both conditions are fulfilled since the film area decreases in transition from the ring to the neck. Therefore, the entire interval $l_0 \in (0, l_{0,s}^*]$ on the curve *3* in Fig. 3c corresponds to the unstable state of the "regular catenoid with a film on one of the rings" system, the latter immediately goes over to the state of singular catenoid (curve *2*).

Even more unexpected features of such a reconstruction of catenoids manifest themselves in the case of asymmetric rings [7]. We go over to analyze this situation.

7. THE CASE OF ASYMMETRIC RINGS

In this case we can set that

$$R_{dn} = 1, \quad R_{up} < 1.$$

The configuration of the regular and singular asymmetric catenoids can be found by simple cutting off by the plane $z = z'$ of the required part from the symmetric catenoid considered above: regular Σ_0 (Fig. 4a) or singular $\Sigma_0^+ \bigcup \Sigma_0^- \bigcup \Sigma_0'$ (Fig. 4b).

We will find the catenoid cross-section $z = z'$ on the interval $0 < z' < l_0/2$ such that the cross-section radius is equal to $R_{up} < 1$. For this purpose we solve the equation for the profile AD of catenoid (4.6) with respect to z

$$AD: \quad z = F(x, a), \tag{7.1}$$

where $F(x, a)$ denotes the function

$$F(x, a) = \frac{a - \operatorname{arccosh}(x \cosh a)}{\cosh a}. \tag{7.2}$$

Setting $x = R_{up}$ in expression (7.1), we find the unknown catenoid cross-section $z = z'$

$$z' = F(R_{up}, a). \tag{7.3}$$

In this case we shall restrict our attention to only those z' which satisfy the condition

$$z' < 0.5 l_0(a).$$

Obviously, this condition imposes an additional constraint on the range of variation in the parameter a

$$a > \operatorname{arccosh}(R_{up}^{-1} \cosh b). \tag{7.4}$$

This narrows the range of variation in the parameter a mentioned above: $a > b$, since the inequality $\operatorname{arccosh}(R_{up}^{-1} \cosh b) > b$ is fulfilled in view of the condition $R_{up} < 1$.

Thus, the unknown catenoid cross-section $z = z'$ on the interval $0 < z' < l_0/2$ such that the cross-section radius is equal to R_{up} is determined by formula (7.3) under condition (7.4). In reality, the area of the catenoid segment between the planes $z = 0$ and $z = z' < l_0/2$ is already found: $S_1 = S(z')$ (see expression (5.2)).

Since the catenoids Σ_0 and $\Sigma_0^+ \bigcup \Sigma_0^- \bigcup \Sigma_0'$ found above are symmetric about the plane $z = l_0/2$, in addition to the cross-section $z = z'$ whose radius equal to R_{up}, found on the interval $0 < z' < l_0/2$, there is an additional cross-section of the same radius on the interval $l_0/2 < z' < l_0$. Thus, the problem of determination of the distance l_1 between the circular rings of radii $R_{dn} = 1$ and $R_{up} < 1$ on the symmetric regular catenoid Σ_0 has two solutions which will be called solution I (without neck) and solution II (with neck) (see Fig. 4a):

$$\text{I}: \quad \begin{cases} l_1 = F(R_{up}, a), \\ S_1 = S(z')|_{z'=l_1}. \end{cases} \tag{7.5}$$

$$\text{II}: \quad \begin{cases} l_1 = l_0(a)|_{b=b_r} - F(R_{up}, a), \\ S_1 = S_0(a)|_{b=b_r} - S(z')|_{z'=l_1}. \end{cases} \tag{7.6}$$

At the same time, in the symmetric singular catenoid $\Sigma_0^+ \bigcup \Sigma_0^- \bigcup \Sigma_0'$ a similar problem has only the solution *II* (see Fig. 4b)

$$\text{II}: \quad \begin{cases} l_1 = l_0(a)|_{b=b_s} - F(R_{up}, a), \\ S_1 = S_0(a)|_{b=b_s} - S(z')|_{z'=l_1}, \end{cases} \tag{7.7}$$

since, in reality, the solution *I* ceases to be the singular solution and becomes the regular solution.

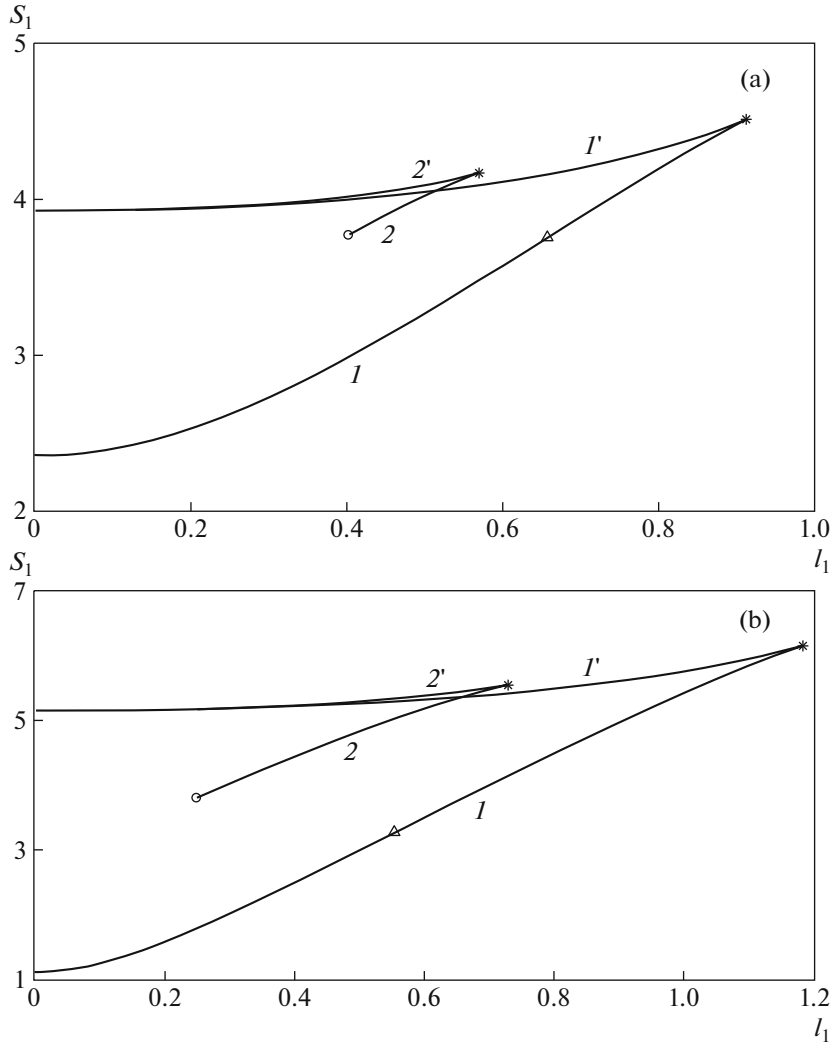

Fig. 5. Area S_1 of the asymmetric catenoid as a function of l_1 in the regular and singular cases at $R_{up} = 0.5$ (a) and $R_{up} = 0.8$ (b). Curves *1* and *2* correspond to the stable branches and *1′* and *2′* to the unstable branches in the regular and singular cases, respectively.

In expressions (7.5)–(7.7) it is necessary to take into account formulas (3.2), (5.2), and (7.2) under condition (7.4).

In what follows, we will give the graphs of the dependences $S_1(l_1)$ calculated from formulas (7.5)–(7.7) for the asymmetric regular and singular catenoids at $R_{up} = 0.5$ (Fig. 5a) and $R_{up} = 0.8$ (Fig. 5b). Curves *1* and *2* correspond to the stable and curves *1′* and *2′* to the unstable branches of the regular and, respectively, singular catenoids.

As before, the asterisks will denote the right-hand ends of the stable branches of the regular and singular catenoids and the corresponding values of the maximum possible $l_{1,r}$ and $l_{1,s}$ will be denoted by $l^*_{1,r}$ and $l^*_{1,s}$, respectively. The symbol ∘ will denote the left-hand end of the stable branch of the singular catenoid defined by constraint (7.4) and the corresponding value of the minimum possible $l_{1,s}$ will be denoted by $l^\circ_{1,s}$.

The value of $l_{1,r}$ at which the neck appears (or disappears) on the regular catenoid will be denoted by $l^\Delta_{1,r}$. The corresponding point on the stable branch $S_1(l_1)$ of the regular catenoid will be denoted by symbol Δ so that when $l_1 < l^\Delta_{1,r}$ the catenoid will have no neck (solution *I*) and when $l_1 \geq l^\Delta_{1,r}$ the catenoid will have a neck (solution *II*) (see Fig. 4a).

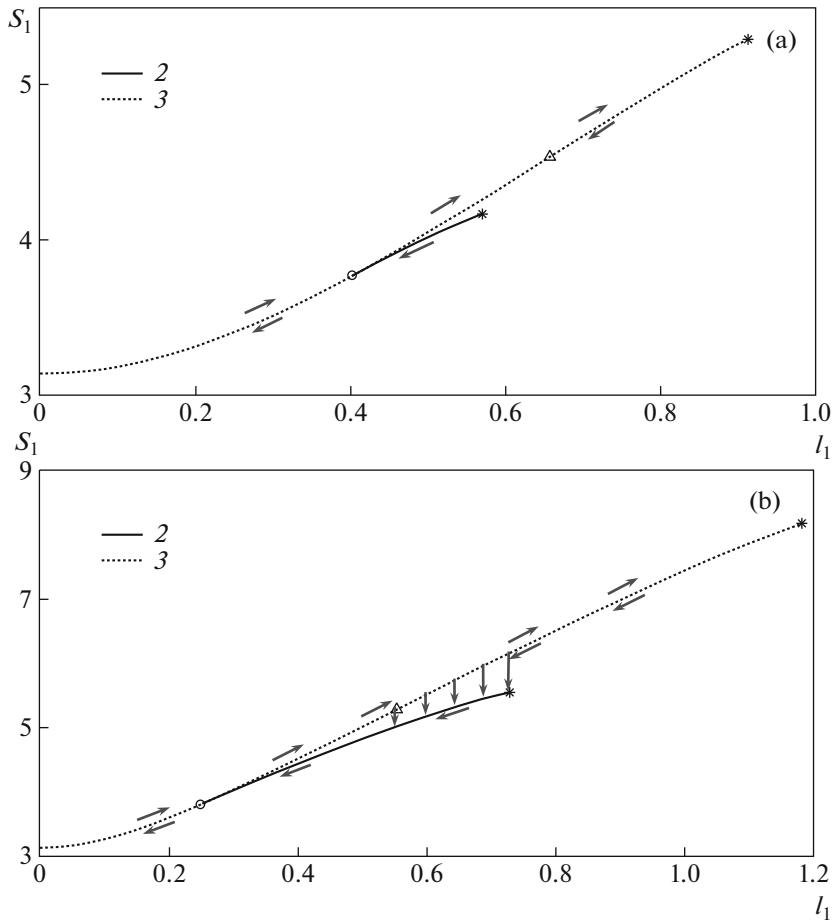

Fig. 6. Stable branches of the dependence of S_1 on l_1 for the asymmetric singular catenoid (curves *2*) and of the dependence of $(S_1 + \pi R_{up}^2)$ on l_1 for the "regular asymmetric catenoid with film on one smaller ring" system (curves *3*) at $R_{up} = 0.5$ (a) and $R_{up} = 0.8$ (b); arrows along the curves denote quasi-stationary variation in the state of system with variation in the distance l_1 and the vertical arrows denote transition of the system from the unstable to the stable position.

It can be seen that for any $R_{up} < 1$ the graphs of $S_1(l_1)$ are qualitatively similar one to another and also they are similar to the initial graph of $S_0(l_0)$ for the symmetric regular and singular catenoid (see Fig. 3c). In addition, similarly to the symmetric case, the regular catenoid cannot spontaneously go over in the singular catenoid since for the latter the dependence $S_1(l_1)$ is always located lower. At the same time, here, as distinct from the case of symmetric rings, continuous inverse transition is possible, namely, with decrease in the distance l_1 between the rings the plane of the middle film of the singular catenoid approaches the plane of the smaller ring and these planes simply coincide at $l_1 = l_{1,s}^{\circ}$. Correspondingly, the film Σ_0' in the neck becomes the film on the upper (smaller) ring and the catenoid itself becomes regular. However, this should be discussed within the framework of analysis of the "regular asymmetric catenoid with the film on the smaller ring" system.

8. THE CASE IN WHICH THE FILM ON THE SMALLER RING IS PLANTED TO THE REGULAR ASYMMETRIC CATENOID

The free energy of the "regular catenoid plus film on the smaller ring" system is proportional to its total area $S_{1,r}(l_1) + \pi R_{up}^2$. We have plotted the graphs of this area as a function of the distance l_1 between the rings (broken curves *3*) for $R_{up} = 0.5$ (Fig. 6a) and $R_{up} = 0.8$ (Fig. 6b). As before, symbol Δ denotes the point of appearance (disappearance) of the neck on the regular catenoid. Curves *2* represent the stable branches for the singular catenoid, the same as those in Figs. 5a and 5b. As before, the left- and right-hand ends of these curves are denoted by symbols ∘ and asterisks.

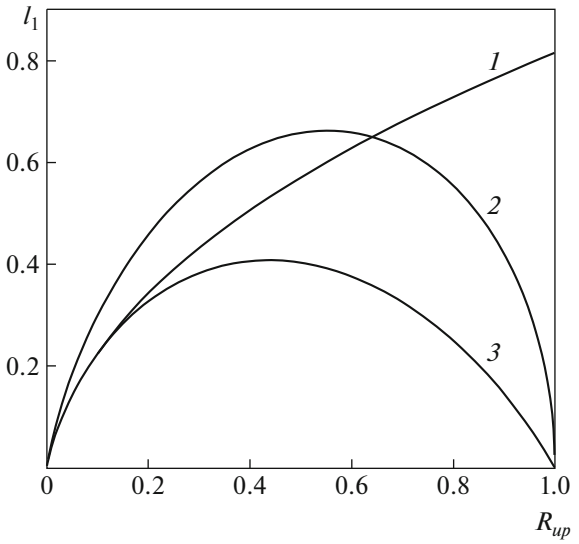

Fig. 7. Quantities $l^*_{1,s}$ (curve *1*), $l^{\Delta}_{1,r}$ (curve *2*), and $l^{\circ}_{1,s}$ (curve *3*) as functions of R_{up}.

As can be seen from Figs. 6a and 6b, with decrease in the distance l_1 between the rings, continuous and even smooth (in the sense of the free energy) transition from the singular asymmetric catenoid to the "regular asymmetric catenoid with film on the smaller ring" system occurs when l_1 reaches the value $l_1 = l^{\circ}_{1,s}$. Clearly, the distance l_1 can decrease further and the system will remain in this stable state. However, what is happened if we begin to increase distance l_1 to $l_1 = l^{\circ}_{1,s}$ and further?

At the first glance, when l_1 reaches the value $l^{\circ}_{1,s}$ the system must choose the most profitable path with the minimum free energy, i.e., go over to the singular asymmetric catenoid, but that is not so [7]. As distinct from the case of symmetric rings, when the regular catenoid always has the neck, in this case the fragments $l_1 \in (0, l^{\Delta}_{1,r}]$ of broken curves *3* in Figs. 6a and 6b correspond to the solution I for the regular asymmetric catenoid (without neck) (Fig. 4a). In order to force the film to slide down from the smaller ring in such a catenoid, it is necessary to increase the film area. In accordance with the two-stage scheme of catenoid reconstruction described in [7], the first stage of restructuring, namely, shedding the film from the smaller ring, turns out to be disadvantageous to the system, since it is associated with expenditure of energy. As a result, the fragments $l_1 \in (0, l^{\Delta}_{1,r}]$ of broken curves *3* in Figs. 6a and 6b will correspond to the metastable state of the system and the system will be indefinitely long time in this state without additional expenditures of energy.

With further increase in l_1, the scenario of the development of events will depend on the radius R_{up} of the smaller ring. At $R_{up} = 0.5$ (see Fig. 6a) the system will remain in the same "regular asymmetric catenoid with film on the smaller ring" state up to the instant at which l_1 reaches the value $l^*_{1,r}$. The pattern will be entirely different at $R_{up} = 0.8$. Here, the value of $l_1 = l^{\Delta}_{1,r}$ is reached earlier than $l_1 = l^*_{1,s}$ (see Fig. 6b). This means that the entire interval $l_1 \in [l^{\Delta}_{1,r}, l^*_{1,s}]$ of broken curve 3 corresponds now to the solution *II* for the asymmetric regular catenoid (with neck) (Fig. 4a). Therefore, the first stage of reconstruction of the regular catenoid to the singular one, namely, shedding the film from the smaller ring to the neck, becomes advantageous to the system and such a reconstruction takes place. Consequently, the entire interval $l_1 \in [l^{\Delta}_{1,r}, l^*_{1,s}]$ of broken curve *3* corresponds now to the unstable configuration.

As a result, if we vary the distance between the rings l_1, either increasing or decreasing it, we can reconstruct the catenoid. The regular catenoid turns into the singular one occurrs at $l_1 = l^{\Delta}_{1,r}$ and reconstruction of the singular catenoid in the regular one occurrs at $l_1 = l^{\circ}_{1,s}$, i.e., hysteresis is observed in the reconstruction of catenoids [7]. Obviously, such hysteresis is possible not always but under the conditions $l^{\circ}_{1,s} < l^{\Delta}_{1,r} < l^*_{1,s}$.

In Fig. 7 we have plotted the graphs of the dependences $l^*_{1,s}(R_{up})$ (curve *1*), $l^{\Delta}_{1,r}(R_{up})$ (curve *2*), and $l^{\circ}_{1,s}(R_{up})$ (curve *3*) obtained as a result of analysis of system (7.5)–(7.7). In particular, the critical value

of $R_{up} \approx 0.641$ for which $l^{\Delta}_{1,r} = l^{*}_{1,s}$ is found. Correspondingly, hysteresis of the reconstruction of the regular catenoid in the singular one and back is possible only if the radius of the smaller ring satisfies the condition $R_{up} > 0.641$. This is in agreement with the results of [7] correct to notation.

SUMMARY

Possible reconstructions of the minimal surface supported by two circular coaxial rings of different radii are fully analyzed. In particular, the surface area (surface energy) as a function of the distance between the rings is plotted for various film configurations. The assumption on metastability of one of the configurations suggested in [7] is justified and the reconstruction hysteresis for a catenoid suggested in [7] is explained to provide a clear physical meaning. The proposed method of analysis based on the methods of the theory of anomalous fluid flow through the porous medium can be extended to the case of non-circular and non-smooth rings.

ACKNOWLEDGMENTS

The work is performed according to the Russian Government Program of Competitive Growth of Kazan Federal University (the first author) and the National Science Foundation IOS-1354956 (the second author).

REFERENCES

1. L. D. Landau and E. M. Lifshitz, *Fluid Mechanics* (2nd Ed.) (Pergamon, 1987; Nauka, Moscow, 1986).
2. J. Plateau, *Statique Experimentale et Theorique des Liquides Soumis aux Seules Forces Moleculaires* (Paris: Gauthier-Villars, 1873).
3. R. Courant, *Dirichlet's Principle, Conformal Mapping, and Minimal Surfaces* (Dover Publications, New York, 2005; Izd. Inostr. Lit., Moscow, 1953).
4. Tchi Dao Chong and A. T. Fomenko, *Minimal Surfaces and Plateau Problem* (Nauka, Moscow, 1987) [in Russian].
5. D. Hoffman and W. H. Meeks, "Minimal surfaces based on the catenoid," The American Mathematical Monthly. Special Geometry Issue (Oct., 1990), **97** (8), 702–730 (1990).
6. G. B. Arfken, H. J. Weber, and F. E. Harris, *Mathematical Methods for Physicists* (Elsevier Acad. Press, Amsterdam, 2013).
7. L. Salkin, A. Schmit, P. Panizza, and L. Courbin, "Influence of boundary conditions on the existence and stability of minimal surfaces of revolution made of soap films," American J. Phys. **82** (9), 839–849 (2014).
8. M. M. Alimov and K. G. Kornev, "Meniscus on a shaped fibre: singularities and hodograph formulation," Proc. R. Soc. A. **470**, 20140113 (2014).
9. M. G. Bernadiner and V. M. Entov, *Hydrodynamic Theory of Anomalous Fluid Flows in Porous Media* (Nauka, Moscow, 1975) [in Russian].
10. S. P. Novikov and A. T. Fomenko, *Elements of Differential Geometry and Topology* (Nauka, Moscow, 1987) [in Russian].
11. V. V. Sokolovskii, "Nonlinear seepage flows of ground waters," Prikl. Mat. Mekh. **13** (5), 525–536 (1949).
12. H. Lamb, *Hydrodynamics* (Cambridge Univ. Press, Cambridge, 1932; Gostekhizdat, Moscow, Leningrad, 1947).
13. S. A. Khristianovich, "Motion of underground waters which does not obey the darcy law," Prikl. Mat. Mekh. **4** (1), 33–52 (1940).
14. S. A. Chaplygin, *Gas Jets* (Gostekhizdat, Moscow, Leningrad, 1949) [in Russian].
15. M. M. Alimov and K. G. Kornev, "An external meniscus on a thin ovoidal fiber (the case of full wetting)," Fluid Dynamics **52** (4), 547–560 (2017).
16. M. A. Lavrent'ev and B. V. Shabat, *Methods of Theory of Functions of a Complex Variable* (Nauka, Moscow, 1973) [in Russian].
17. M. I. Gurevich, *Theory of Jets in Ideal Fluids* (Academic Press, New York, 1965; Nauka, Moscow, 1979).
18. V. I. Smirnov, *Course of Higher Mathematics*, Vol. 1 (Nauka, Moscow, 1974) [in Russian].

Translated by E.A. Pushkar